Regular Article

ANALYTICAL
AND BIOANALYTICAL
CHEMISTRY
RESEARCH

Published by the
Iranian Chemical Society

Anal. Bioanal. Chem. Res., *Vol. 10, No. 1, 71-86, January 2023.*

Synthesis of Ternary Complex-Based Ion Imprinted Polymer Sorbent for Selective Adsorption of Lead Ions

Novita Ambarsari[a,*], Muhammad Ali Zulfikar[b] and Muhammad Bachri Amran[b]

[a]*Analytical Chemistry Division, Faculty of Mathematics and Natural Sciences, Institut Teknologi Bandung, Indonesia. National Research and Innovation Agency (BRIN), Indonesia*

[b]*Analytical Chemistry Division, Faculty of Mathematics and Natural Sciences, Institut Teknologi Bandung, Indonesia*

(Received 7 June 2022, Accepted 13 September 2022)

In this study, Pb^{2+} ion imprinted polymer particles were synthesized by preparing a ternary complex of lead imprinted ions with 4-(2-pyridilazo) resorcinol and 4-vinyl pyridine. Pb-IIPs as sorbents with ternary complexes between Pb^{2+}, PAR, and 4-VP as template carrier molecules had not been previously reported. The ternary complex formed was then copolymerized with methacrylic acid as a functional monomer, Trimethylolpropane trimethacrylate as a crosslinking agent, methanol as porogen, and benzoyl peroxide as initiator. Polymerization was carried out by the thermal method. HNO_3 5 M was used to remove the template ion by shaking the polymer for 24 h several times to obtain leached IIP particles (Pb-IIPs). Non-Imprinted Polymers (NIPs) as control were similarly prepared without imprinted ions. In this study, two types of NIPs were made including with and without the addition of PAR ligands (NIP and NIPP). All polymer particles were characterized by spectral (FTIR), thermal (TGA-DTG), morphology (SEM), and nitrogen adsorption studies (BET). The adsorption and selectivity studies for lead ions were carried out with Pb-IIP, NIPP, and NIP. The adsorption of 20 mg l^{-1} of Pb^{2+} using 25 mg of polymer particles in pH 6 with an interaction time of 90 min. The maximum adsorption capacity of leached Pb-IIP was found to be 14.3 mg g^{-1} which is higher than the NIPP and NIP. The Pb-IIPs displayed excellent selectivity against three common divalent ions Cu^{2+}, Cd^{2+}, and Zn^{2+} with selectivity coefficients of 19.98, 42.15, and 42.96, respectively, showing high anti-interfere ability. The precision for the method was determined by the percentage of relative standard deviation (RSD) to be 2.9% for five times the replication of the adsorption measurement. The spike and un-spike samples method was conducted to assess the accuracy of the Pb-IIP adsorption which shows a high percentage of recovery values ranging from 97-103%, indicating its accuracy.

Keywords: Lead, Ion imprinted polymer, Heavy metal, Selective adsorption, Separation

INTRODUCTION

Pollution by heavy metals in the environment is still an important problem and become a worldwide concern in recent decades, especially because they can cause various health problems and can accumulate in the food chain. Their characteristics have high toxicity even in very low concentrations, non-biodegradability, and very large distribution entering the water and various food chain routes, for example in the human body through drinking water, food, and inhaling particulates in the air [1-3]. Of all the harmful metal ions, lead (Pb) is one of the most widespread metal ions in the environment due to the nature of lead that can be emitted into the atmosphere from the burning of fossil fuels and other processes. Some industrial activities such as the battery, paperboard mill, pulp, industrial ammunition, pigment manufacturing, and coal burning become another source of lead pollution in the environment [3-6].

Unlike organic compounds, lead cannot be degraded biologically, and accumulates by association with other

*Corresponding author. E-mail: novitaambar@gmail.com

inorganic and organic compounds, for example through adsorption processes, complex formation, or chemical combinations [7-9]. Analytical methods of measuring Pb can be carried out using several instruments such as Flame Atomic Absorption Spectrometry (FAAS), Electrothermal Atomic Absorption Spectrometry (ETAAS), Graphite Furnace Atomic Absorption Spectrometry (GFAAS), Inductively Coupled Plasma Atomic Emission Spectrometry (ICP-AES), and Inductively Coupled Plasma Mass Spectrometry (ICP-MS). The most widely used instrument is FAAS but the direct determination of Pb at very small concentrations is usually difficult due to the lack of sensitivity of the instrument and the presence of other matrix disturbances in the sample [10-12]. Therefore, the development of analytical methods that are sensitive and selective and can minimize interference with Pb measurements in various samples is an important requirement at this time. Preliminary preconcentration and matrix removal steps for different environmental samples are highly needed to ensure accuracy and precision [10,13-14].

Solid Phase Extraction (SPE) is mostly used as a superior method for preconcentration and separation of lead and other toxic metal ions that has simplicity, small consumption of organic solvent, and low-cost preparation but it has poor selectivity [15-17]. SPE linked with Ion Imprinted Polymers (IIPs) can improve the selectivity and sensitivity of SPE. IIPs are polymeric materials that have specific active sites for the targeted ions [18-19]. IIPs are the development of the key and lock model which was first introduced by Nishide *et al*. (1976) after previously being introduced to MIP in 1972 by Wulff and Klotz [20-22]. IIPs have several advantages including having a specific cavity for the target (ion), good stability in various media, relatively easy to synthesize, natural specificity, cost-effectiveness, and being highly reusable many times. It can be stored for a long time without losing its affinity [23-25].

The preparation procedure of IIPs in general consists of the formation of a ligand-metal complex followed by copolymerization in the presence of an excess of a cross-linking agent. After the polymer is formed, the template ion is removed and leaves three-dimensional recognition cavities within the polymer network with a predetermined orientation according to their stereochemical interaction with the template metal ion [26-28]. Different methods to synthesize an IIP were classified into four approaches: (1) linear chain polymers carrying metal-binding groups were crosslinked with a bifunctional reagent in presence of metal ions, (2) chemical immobilization of ligands with a vinyl group to form binary complexes of metal ions in the presence of a cross-linker, (3) surface imprinting involving a ligand having or not a vinyl group, and (4) trapping of a non-vinylated ligand or mixed of non-vinyl and vinyl ligand to formed binary/ternary complexes of metal ions inside a polymer network [29].

For its simplicity, the trapping approach using a non-polymerizable ligand was the most commonly used technique for the synthesis of IIP for many metal ions. Several studies on IIPs that have been carried out previously used the trapping method with ternary complexes ion formation for various metal ions [18,26,30-37]. The stoichiometry of the ternary complex was established using the mole ratio and continuous variation method [36]. Metilda *et al*. (2004) have described the effect of IIP with ternary mixed ligands complex produce a higher percent enrichment value compared to IIP with individual binary complexes probably due to the availability of more interaction points, hence more number of easily accessible sites due to ternary complex [37]. Several studies on Pb-IIPs that have been carried out previously used various chelating agents and monomers including MAA and 4-VP [13], 1-vinyl imidazole and TMSPMA [6], vinyl imidazole [5], and methacrylic acid and pyridilazo naphthol (PAN) [4] for the separation and preconcentration of Pb in various samples.

In the present work, we report the synthesis of Pb-IIPs with trapping techniques involving the Pb(II) ternary complex with PAR and VP ligands. 4-(2-Pyridilazo) resorcinol (PAR) is very sensitive and is widely used for the colorimetric determination of metal ions. PAR is a compound with an azo group that is soluble in water and acts as a chelating agent in metal ion analysis and forms soluble complexes with many metals. Complex formation with PAR is rapid and has high stability constant [38]. The vinyl groups in VP will covalently bind with the polymeric backbone during polymerization, while the PAR ligands will be trapped inside the polymer matrix. The type of ligand used and the ability of the polymer to maintain the geometric structure of the mold, affect the ability of adsorption and selectivity of IIPs [39]. The desired Pb-IIPs show greater selectivity

towards Pb^{2+} over Cd^{2+}, Cu^{2+}, and Zn^{2+} ions.

EXPERIMENTAL

Chemical Reagents

All chemicals used in this study were of analytical reagent grade. Every aqueous solution was prepared using deionized water. Lead acetate was dissolved and diluted with deionized water to prepare a stock solution of 1000 mg l^{-1} of Pb^{2+}. The pH of the solution was adjusted to the appropriate value by 0.001 M and 0.01 M HNO_3/NaOH solutions. $Pb(CH_3COO)_2.3H_2O$, methacrylic acid (MAA), 4-vinyl pyridine (4-VP), 2,2'-4-(2-pyridilazo) resorcinol (PAR), Trimethylolpropane trimethacrylate (TRIM), and benzoyl peroxide (BPO) were obtained from Sigma-Aldrich. All reagents used in the present study were of analytical grade.

Instrumentation

An atomic Absorption Spectrometer double beam GBC-Avanta 6506 was used for measuring Pb^{2+} ion concentration. A Mettler-Toledo pH meter was used for pH solution determinations. Fourier transform infrared (FT-IR) spectra were recorded by the KBr pellet method using The FTIR Prestige-21 (Shimadzu, Japan) over the wave number range 4000-400 cm^{-1}. The surface morphology, size, shape, and atomic composition were examined by Scanning Electron Microscope (SEM)-Energy Dispersive X-Ray Spectroscopy (EDS) (SEM SU 3500). Surface area and porosity analyzer with Quadrasorb Evo QDS-MP-30 were used to analyze Brunauer, Emmet, and Teller (BET) specific surface area and pore size of the adsorbent.

Synthesis of Ion Imprinted Polymer

The synthesis of IIP particles was carried out with the Bulk method in two steps: (i) ternary complex formation, and (ii) copolymerization of a ternary complex with methacrylic acid (functional monomer) and Trimethylolpropane trimethacrylate (crosslinking monomer).

The ternary complex of Pb^{2+} ion with 4-(2-pyridilazo) resorcinol (PAR) and 4-vinyl pyridine (4-VP) was prepared by stirring a mixture of 1.0 mmol of lead acetate, 1.0 mmol of PAR, and 2 mmol of 4-VP in 10 ml methanol for 2 h. The formation of the ternary complex was confirmed by UV-Vis spectral studies [27,34,40]. Absorption spectra of methanol solution of Pb^{2+} + PAR, Pb^{2+} + VP, and Pb^{2+} + PAR + VP is shown in Fig. 1a. The ternary complex of Pb^{2+} + PAR + VP

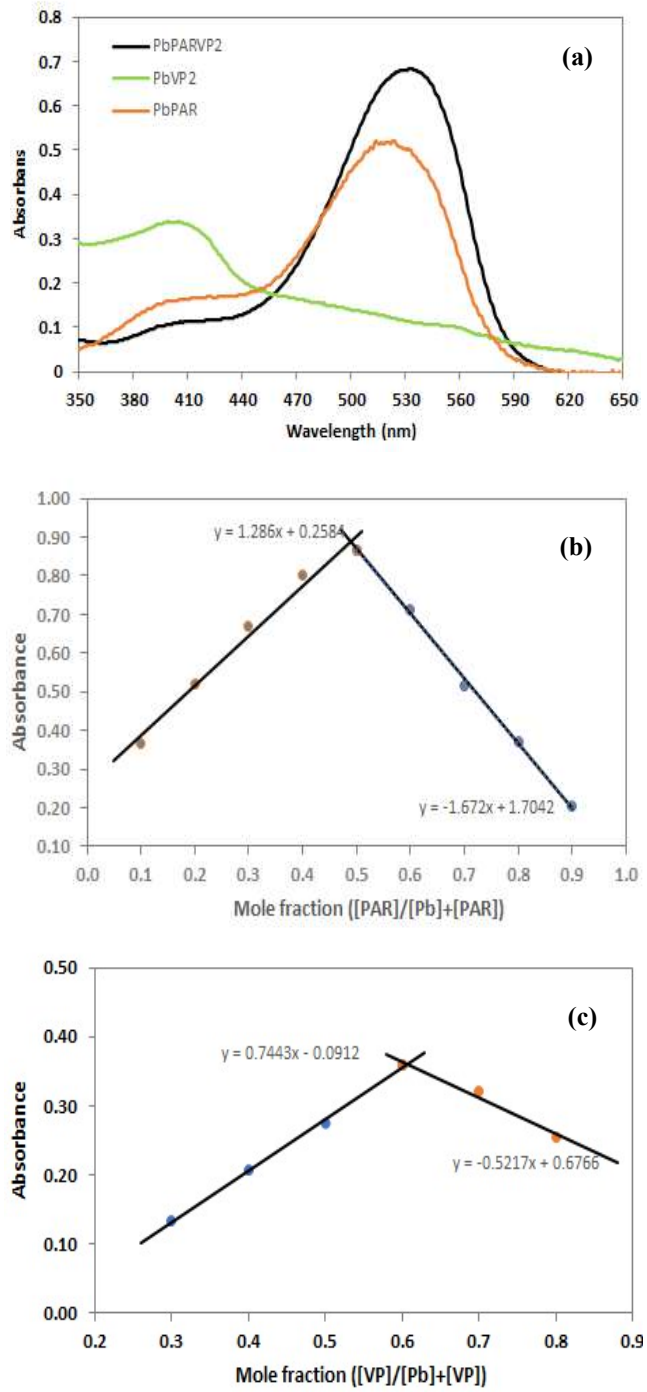

Fig. 1. (a) UV-Vis absorption spectra of complex [PbPAR], $[Pb(VP)_2]$, and $[PbPAR(VP)_2]$ in methanol. Job's plot for (b) [PbPAR], (c) $[Pb(VP)_2]$ complex formation.

is formed and can be seen from the spectra that show a maximum absorption of around 534 nm. The ratio of the mole fraction of the ternary complex Pb^{2+} + PAR + VP from Job's plot as shown in Fig. 1b and 1c was obtained by using the continuous variation method [40]. As can be seen from Fig. 1c and 1d, the maximum absorption of Pb^{2+} + PAR and Pb^{2+} + VP occurs at the mole fraction of [Pb]/{[Pb]+[PAR]} and [Pb]/{[Pb]+[VP]} 0.5 and 0.6, respectively. This result shows that the stoichiometry of the ternary complex is 1:1:2 [36].

The ternary complex thus prepared was imprinted in MAA and TRIM. For polymerization, 6 mmol MAA, 30 mmol TRIM (crosslinker), and 100 mg of BPO were added and stirred until a homogenous solution was obtained. The mixture was purged with N_2 gas for 10 min and heated at 70 °C with stirring at 200 rpm for 2 h. The material was thus obtained was ground and sieved to get the particle sizes between 60-80 mesh. The Pb^{2+} ion as imprint ion was leached from the polymer by stirring with HNO_3 5 M solution for 24 h, in 3-5 cycles. After all the Pb^{2+} ion was leached out, the Pb-IIPs were then washed with demineralized water. The non-imprinted polymer was prepared in similar steps as that of Pb-IIPs except that target ions were not added but with PAR ligand added (NIPP) and without PAR ligand added (NIP). Pb-IIPs (before and after leaching) and the NIPs and NIPPs were characterized by FTIR, SEM, and BET. The synthesis procedure is illustrated in Fig. 2.

Batch Sorption Experiment

The batch experimental procedure was employed for the adsorption of Pb^{2+} from an aqueous solution. 25 mg of Pb-IIPs was placed in a 50 ml Erlenmeyer flask and then left to interact with 25 ml of 20 mg l^{-1} Pb^{2+} at pH 6 and the mixture was shaken at 150 rpm for 90 min of interaction. All the filtrate was then measured by FAAS. The same procedure was also carried out with the NIPPs and NIPs. The adsorption capacity was calculated as follows:

$$qe = \frac{(Ci-Cf)V}{m}$$

Where qe is the adsorption capacity (mg g^{-1}), V is the volume of solution (l), Ci is the initial concentration of Pb^{2+} (mg l^{-1}), Cf is the final concentration of Pb^{2+} (mg l^{-1}), and m is the Pb-IIPs mass (g).

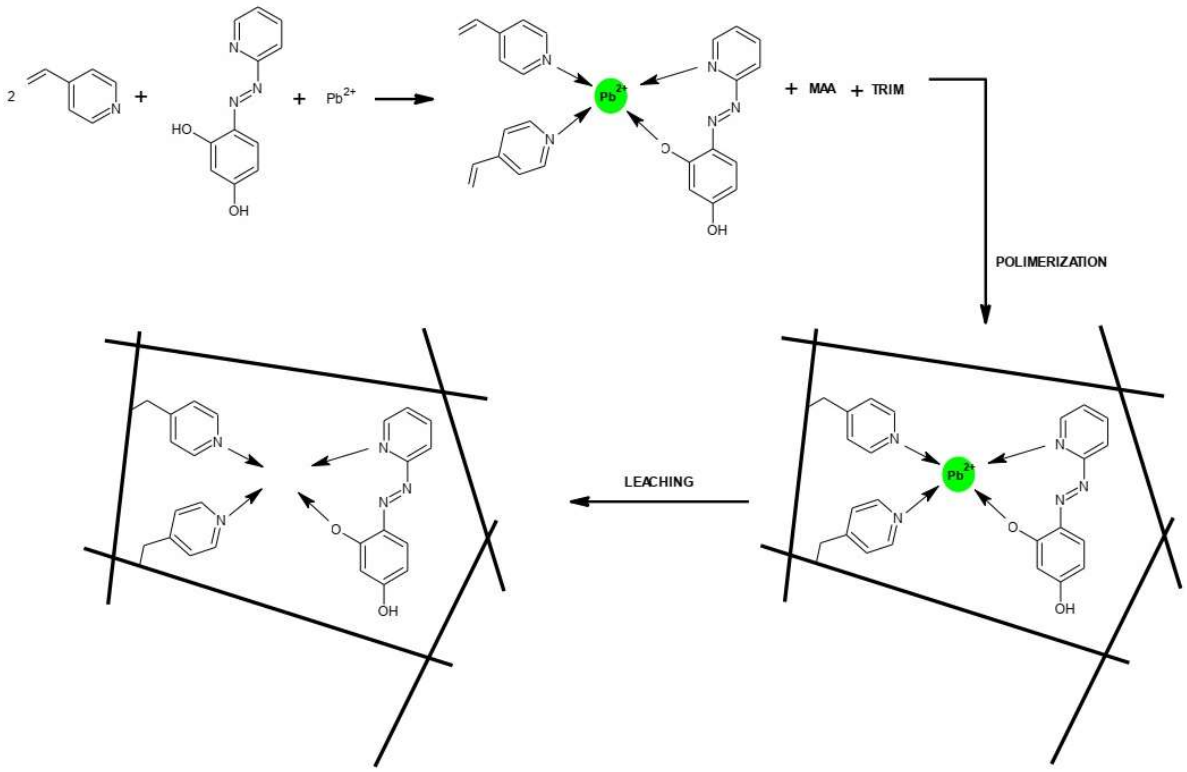

Fig. 2. Schematic procedures of ternary complex-based Pb-IIP synthesis.

pH Optimization

to evaluate the effect of pH on the sorption of Pb^{2+} by Pb-IIP, 25 mg Pb-IIP was placed in five of 50 ml Erlenmeyer flasks and then interact with 25 ml of Pb^{2+} 20 mg l^{-1} for 3 h and shaken in 150 rpm shaker with different pH value for 3, 4, 5, 6, and 7 at room temperature. The filtrate was separated from the sorbent and analyzed by FAAS to measure the Pb^{2+} ions concentration. HNO_3/NaOH 0.001 and 0.01 M, respectively were used to set the pH value of the mixture. Under the same condition, the NIPPs and NIPs were also examined by the same procedure.

Effect of Interaction Time on Sorption

The effect of interaction time on sorption was investigated by contacting 25 mg Pb-IIP which was placed in nine 50 ml Erlenmeyer flasks and then interact with 25 ml of Pb^{2+} 20 mg l^{-1} at optimum pH and shaken in a 150 rpm shaker at room temperature. Interaction time was set for 5, 10, 20, 30, 60, 90, 120, 150, and 180 min. Subsequently, the mixture was filtered and measured for Pb^{2+} ions concentration by FAAS.

Adsorbent Dose Optimization

Adsorbent dose optimization was studied by contacting Pb-IIP with 25 ml Pb^{2+} 20 mg l^{-1} at optimum pH and interaction time in a 50 ml Erlenmeyer flask and shaking in a 150 rpm shaker at room temperature. Sorbent mass was set for 25, 30, 35, 40, 45, and 50 mg. The filtrate was separated from the sorbent and measured for Pb^{2+} ions concentration by FAAS. Under the same condition, the NIPPs and NIPs were also examined by the same procedure.

Determination of Maximum Adsorption Capacity

To determine the maximum adsorption capacity of the sorbent, 25 mg Pb-IIP was placed in a 50 ml Erlenmeyer flask and then interact with 25 ml of Pb^{2+} at optimum pH, interaction time, and adsorption dose. The mixture was shaken in a 150 rpm shaker with various concentrations of Pb^{2+} for 5, 10, 15, 20, 25, 30, 35, and 40 mg l^{-1}. The filtrate was separated from the sorbent and measured for Pb^{2+} ions concentrations by FAAS. NIPPs and NIPs were also treated with the same procedure as controls.

Selectivity Test

The selectivity of Pb-IIPs sorbent to Pb^{2+} ions was determined by interacting 25 mg of the sorbent in 25 ml of single, binary, and quaternary mixtures of Pb^{2+}, Cu^{2+}, Cd^{2+}, and Zn^{2+} metal ions at a concentration of 0.00965 M each. The ion recognition capacity of Pb-IIP materials is well-reflected by Pb^{2+} selectivity in the presence of other competing ions.

The following equation was employed to evaluate the selectivity of the Pb-IIP, NIPP, and NIP:

$$K_d = ((C_i-C_f)/C_i)(V/W)$$

$$k = K_{dPb}/K_{dMe}$$

$$k' = k_{imprinted}/k_{non\text{-}imprinted}$$

where K_d, k, and k' represents the distribution ratio, selectivity coefficient, and relative selectivity coefficient. K_{dPb} and K_{dMe} show the distribution ratio for the Pb^{2+} ion and the other selected competitive metal ion respectively.

RESULTS AND DISCUSSION

Characterization

The Fourier Transform Infrared (FT-IR) spectra for Pb-IIP before and after the leaching process, NIPPs, and NIPs are demonstrated in Fig. 3. The absorption at wave number 2974 cm^{-1} in the IR NIP spectrum is thought to come from MAA, TRIM, and 4-VP, each of which has a $-CH_3$ group. The success of the polymerization process can be seen, one of which is the loss of the vibrational absorption peak of the C=C double bond which turns into a C-C single bond after the polymer is formed [41]. However, the IR spectrum obtained still shows a peak at a wave number of 1637 cm^{-1} in the NIP spectrum. This peak can be thought to originate from the C=N or C=C (pyridine ring) vibrations of 4-VP which also acts as a functional monomer. However, another possibility is that the peak comes from the presence of the C=C double bond vibration due to the excess amount of monomer (MAA) or crosslinker (TRIM) which does not react during polymerization [4,42]. The IR spectrum of NIPs-PAR showed a similar spectral pattern to that of NIPs. The presence of PAR was detected from the presence of a peak at wavelength 1386 originating from the C-N bond.

IR spectrum of Pb-IIPs (before and after leaching) and

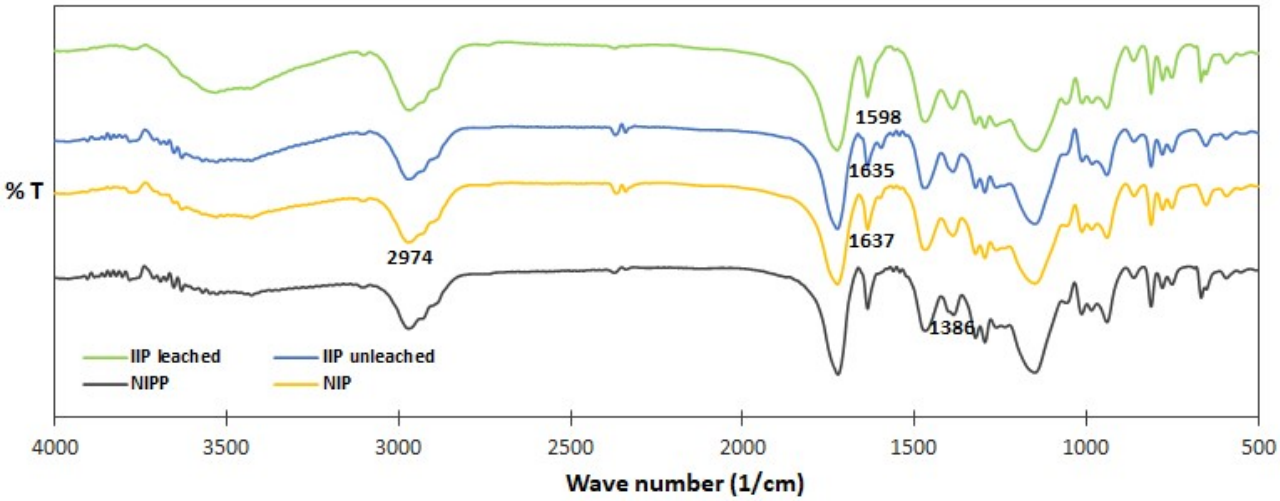

Fig. 3. FT-IR spectra of NIPPs, NIPs, Pb-IIP unleached, and Pb-IIP leached.

non-imprinted polymers (NIPP and NIP) shows similarities to each other which means that the three polymers have the same basic framework. The absorption at a wavenumber of 1598 cm^{-1} in the Pb-IIPs spectrum before leaching, shows Pb-O vibrations which are thought to originate from the coordination side of Pb ions with PAR ligands [43]. This peak was not found in NIPP, NIP, and Pb-IIPs after leaching. The IR spectrum could not clearly identify the coordination of Pb metal ions with the 4-VP ligand. However, the typical absorption peak from the pyridine ring vibration of 4-VP was still found in the IR spectrum of Pb-IIPs before and after leaching.

A Scanning Electron Microscopy (SEM) image for the four types of sorbents with a magnification of 20,000x is shown in Fig. 4. The picture shows that the surface of Pb-IIP polymer before leaching is denser than Pb-IIP after leaching which has a more hollow surface due to Pb^{2+} ions having been released from the polymer. The picture also shows the surface of the NIPP which looks different from the NIP. NIPP has an agglomerate-like surface probably due to the presence of PAR ligands that participate in filling the polymer surface.

The results of elemental analysis from Energy Dispersive X-ray (EDX) measurements for Pb-IIP before leaching and after leaching, NIPP, and NIP are shown in Table 1. Based on the table, it can be seen that element C, O, and N is the main constituent of the four types of sorbents. The table shows that Pb was found in the Pb-IIP sorbent before leaching. This indicates that the Pb^{2+} ion as a template in Pb-IIP has been successfully bound to the carrier complex, namely $[Pb(PAR)(VP)_2]$ and the leaching process in Pb-IIP has been going well because no more Pb elements were found in the Pb-IIP sorbent after leaching.

Surface area and pore size analysis values for leached Pb-IIP and the NIPs (NIPP and NIP) are shown in Table 2. Surface area, pore volume, and pore size for leached IIP are higher compared to the NIPs, which shows the effect of the template ion imprinting process in polymer Pb-IIP. Further, the average pore diameter for leached IIP is in the range of 20-30 A indicating that polymer materials with nanopores were obtained in the present study.

Thermogravimetric analysis (TGA) and Differential Thermal Gravimetry (DTG) curves of IIPs before and after leaching, NIPPs, and NIPs to evaluate the thermal stability of the polymer particles were shown in Fig. 5. According to the thermogram of TG-DTG for all polymers, there are several stages of decomposition that occur. A very clear difference is seen in the thermogram of the unleached IIPs which shows the initial decomposition temperature is around 250 °C, earlier than others, possibly due to the presence of the Pb-PAR complex.

TG-DTG curves for NIPP also show a slight decomposition process at a temperature around 250 °C which is possibly related to the presence of PAR ligands in the polymer matrix. No thermal decomposition occurs until 280 °C for other polymers. In all polymers, reduction of mass until ~100 °C has resulted from the evaporation of the solvent

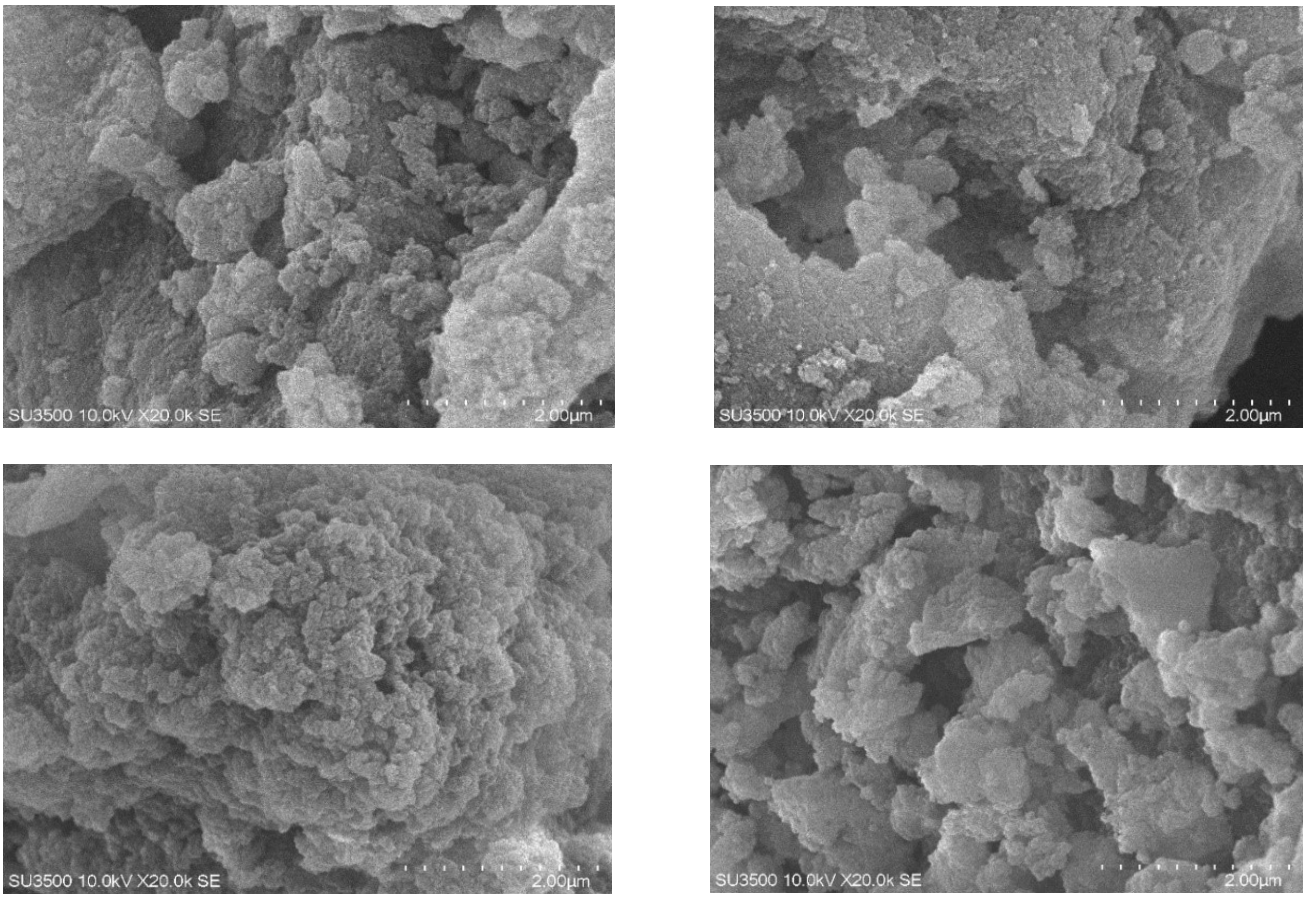

Fig. 4. The SEM images of (a) Pb-IIP unleached, (b) Pb-IIP leached, (c) NIPPs, and (d) NIPs.

Table 1. Elemental Analysis from SEM-EDX Analyzer for all the Polymers

	%Mass				%Atom			
Sorbent	C	N	O	Pb	C	N	O	Pb
Pb-IIP leached	59.68	14.13	26.19	0	65.25	13.25	21.5	0
Pb-IIP unleached	56.63	16.65	25.43	1.29	62.87	15.85	21.2	0.08
NIPP	59.94	16.12	23.94	0	65.34	15.07	19.59	0
NIP	57.4	16.89	25.7	0	62.95	15.89	21.16	0

Table 2. Surface Area and Pore Size Analysis Data of Leached IIP and the NIPs (NIPP and NIP)

Sorbent	Surface area (m^2 g^{-1})	Pore volume (cm^3 g^{-1})	Pore size (× 10 A)
IIP leached	11.01	0.016	2.878
NIPP	7.94	0.008	1.624
NIP	5.48	0.007	1.629

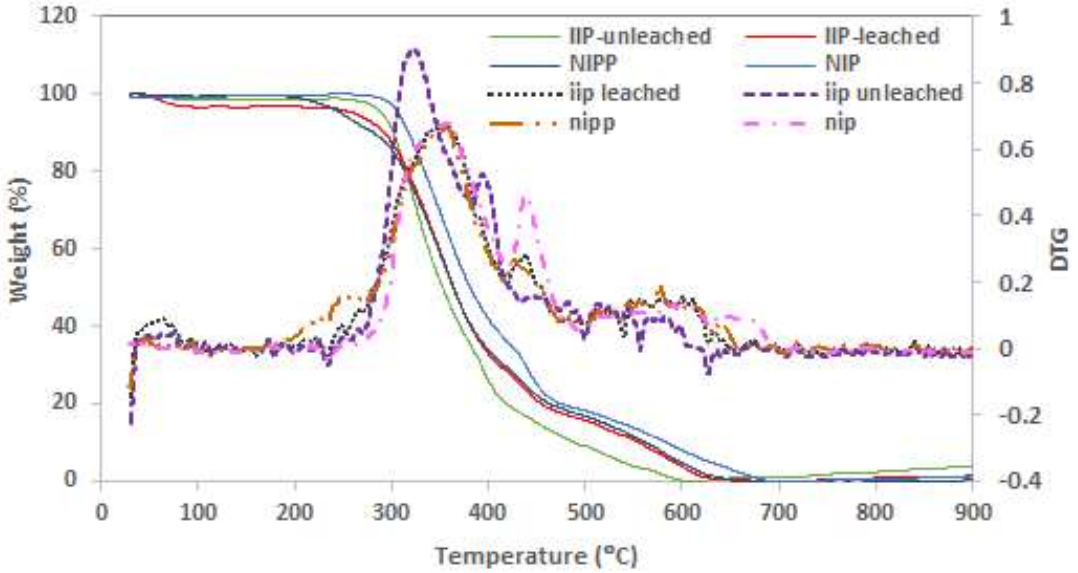

Fig. 5. The TGA and DTG curves for IIP before leaching, IIP after leaching, NIPP, and NIP.

bounded in the structure of the polymer. Reduction of mass with maximum value occurs at temperatures 300-400 °C reaching 80% as a result of the decomposition of the carboxyl compounds contained in the polymer. Above the temperature of 400 °C decomposition occurs including the main chain break of the remaining polymer [44-45]. All polymer materials show good thermal stability and decompose completely at a temperature of 600°C. Thermogram TG-DTG for IIP leached, NIPPs, and NIPs shows a similar pattern that indicates the leaching process of template ion has been successful.

pH Optimization

The effect of the pH of the Pb^{2+} solution on the adsorption capacity of Pb-IIPs is shown in Fig. 6. The test was carried out by placing 25 mg of Pb-IIP and 25 ml of a 20 mg l^{-1} Pb^{2+} solution which had been adjusted at pH 3 to 7 in an Erlenmeyer flask and then stirred for 3 hours. The solution was then separated from the polymer and the Pb^{2+} concentration was measured using FAAS. The optimum adsorption capacity (Q) for each polymer was obtained at pH 6 with a Q value of Pb-IIP reaching 10.06 mg g^{-1}.

The adsorption capacity of the Pb-IIP increased with increasing pH probably due to reduced competition from H^+ ions in solution, so that more Pb^{2+} ions could be adsorbed by the polymer. In addition, at a pH of less than 6, the presence

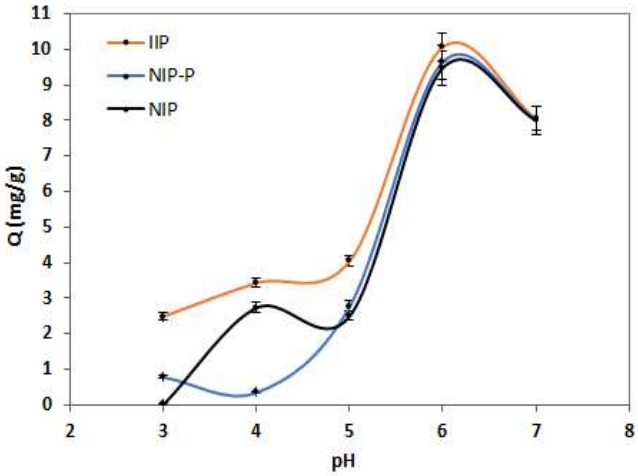

Fig. 6. Effect of pH on adsorption capacity of Pb-IIPs.

of abundant H^+ ions in the solution causes the active group on the sorbent to be protonated, resulting in repulsion with Pb^{2+} ions which are also positively charged. At a pH greater than 6, the adsorption capacity of the polymer decreased due to the hydrolysis of Pb^{2+} ions into $Pb(OH)_2$ in the solution.

Figure 7 shows the zeta potential value of Pb-IIP in the condition of pH solutions 2, 4, 6, 8, and 10. The results show that at pH below 4, the zeta potential of Pb-IIP obtained was +15.4 mV, which means at this condition there was a repulsion force between the Pb^{2+} ion with the Pb-IIP

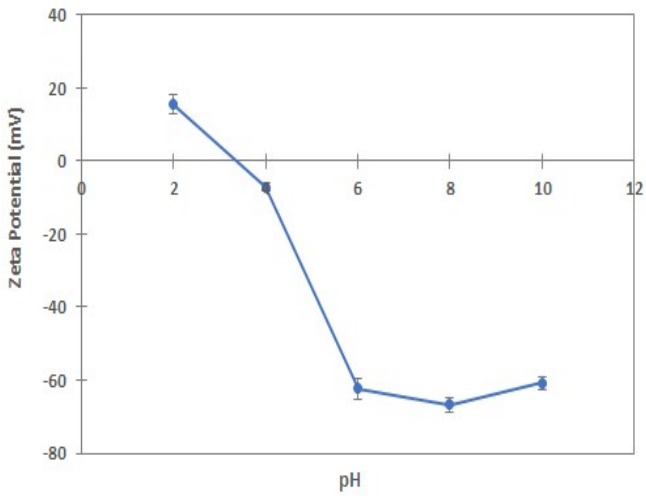

Fig. 7. Zeta potential of Pb-IIPs in various pH.

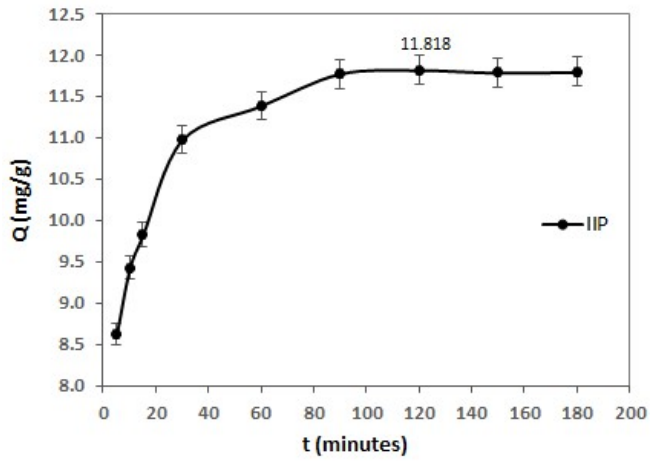

Fig. 8. Effect of contact time on adsorption capacity of Pb-IIPs.

particles. At pH more than 4, the zeta potential of the Pb-IIP obtained was negative values and reach -62.4 mV at pH 6.

This indicates the sufficient for strong electrostatic attraction between the template ion with the Pb-IIP. There are no significant differences in zeta potential value at pH 8 and 10. The profile of the zeta potential value is in accordance with the results of pH optimization which show that the optimum pH is reached at pH 6.

Contact Time Optimization

Determination of the optimum adsorption contact time of Pb-IIP with a sorbent mass of 25 mg at a concentration of 20 mg l^{-1} Pb^{2+} solution at pH 6 obtained the optimum contact time of 120 min or 2 h as shown in Fig. 8 with adsorption capacity value (Q) of Pb-IIP was 11.82 mg g^{-1}. At the contact time of 5 to 30 min, there was a very significant increase in adsorption on the IIP sorbent because the number of binding sites was still available in very large quantities. The adsorption process in IIP reached equilibrium at a contact time of 120 min because all the binding sites were filled with Pb^{2+} ions.

Contact time in the adsorption process is important to study to determine the time required for a metal ion to bind to the active site on the sorbent. This is mainly because the active site on the IIP sorbent is not always on the surface of the sorbent so metal ions need time to move and bind to the active site on the polymer [18].

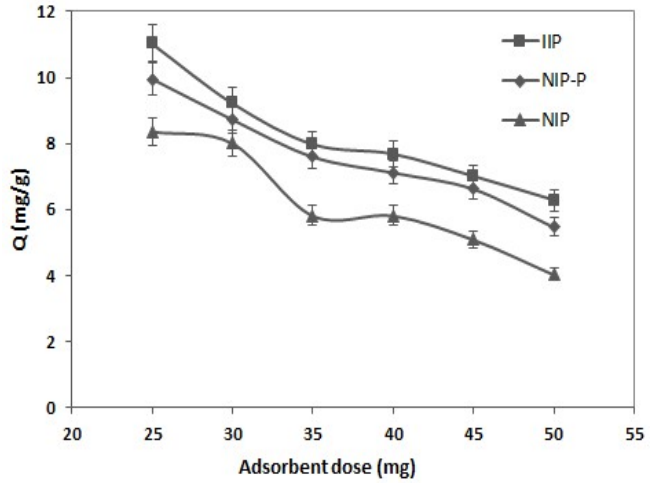

Fig. 9. Effect of sorbent dose on adsorption capacity of Pb-IIPs.

Adsorbent Dose Optimization

The effect of polymer mass on the adsorption capacity of the sorbent is shown in Fig. 9. The mass of the sorbent used for the adsorption process was from 25 mg to 50 mg with a concentration of Pb^{2+} solution of 20 mg l^{-1} at the optimum pH and contact time. The value of the adsorption capacity of the sorbent decreased with the increase in the mass of the sorbent used for the Pb^{2+} ion adsorption process. The sorbent mass of 25 mg was used for the adsorption process in this study because it gave the best adsorption capacity value of

11.04 mg g^{-1}.

The optimization of the IIP sorbent mass used in the adsorption process is important to study because it can describe the capacity of the sorbent to a metal ion at a certain concentration. The result shows that the adsorption capacity as the sorption mass per unit of the sorbent decreases, with the increase of the adsorbent doses. But, the percentage of adsorption increased. The decrease in the value of adsorption capacity with an increase in the mass of the sorbent used occurred due to the increase in the number of active sites that remained unsaturated on the sorbent that did not interact with Pb^{2+} [1].

Effect of Initial Concentration on Adsorption capacity of Pb-IIP, NIPP, and NIP

Effect of initial concentration of Pb^{2+} solution to determine the maximum adsorption capacity of Pb-IIP sorbent in the adsorption process with a mass of 25 mg NIP, NIPP, and Pb-IIP sorbents which were contacted with Pb^{2+} solution at a concentration of 5; 10; 15; 20; 25; 30; 35; and 40 mg l^{-1} at pH 6 for 120 min. The curve of the effect of the concentration of Pb^{2+} solution on the maximum adsorption capacity of IIP, NIPP, and NIP for each polymer composition is shown in Fig. 10.

The adsorption capacity increased with the increase in the concentration of the Pb^{2+} solution until there was no further change, indicated by a horizontal curve. The increase in adsorption capacity may be caused by the mass transfer driving force which increases with increasing Pb^{2+} concentration so that the adsorption performance increases. However, the experiment could not be continued because at high concentrations there was precipitation of Pb^{2+} ions at pH 6 as can be seen in the initial concentration of Pb^{2+} 40 mg l^{-1}, and the adsorption capacity of all the sorbents was decreased. The adsorption capacity of Pb-IIP was 14.30 mg g^{-1}, while NIPP and NIP had adsorption capacities of 12.56 mg g^{-1} and 10.63 mg g^{-1}, respectively. The difference in the adsorption capacity of IIP and each of these NIPs indicates the role of ion imprinting in determining the adsorption capacity of an adsorbent. The ion-binding area generated by the imprinting process in IIP forms the basis for surface activation of the polymer to absorb ions extensively, whereas in NIP (and NIPP) it lacks ion recognition regions and remains non-specific [32]. The NIPP and NIP sorbents have a maximum

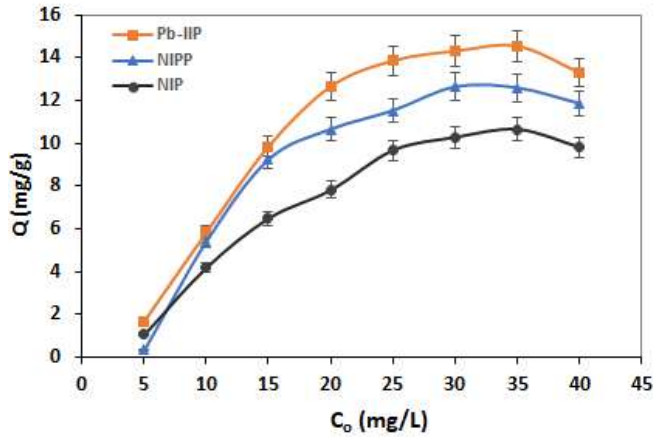

Fig. 10. Effect of initial concentration on adsorption capacity of Pb-IIP, NIPP, and NIP.

adsorption capacity that is not much different from IIP because MAA, TRIM, and 4-VP have several functional groups that can interact with Pb^{2+} ions, but without a specific template, as found in Pb-IIP. NIPP and NIP do not have a better ability to recognize Pb^{2+} ions.

Adsorption Isotherm

To determine the type of Pb^{2+} ion adsorption on Pb-IIP polymers, the Langmuir and Freundlich adsorption isotherm linear model was used. The adsorption mechanism was determined by using 25 mg sorbent in 25 ml of Pb^{2+} solution of varying concentrations from 5 mg l^{-1} to 40 mg l^{-1} at 25 °C temperature.

The Langmuir adsorption isotherm models are expressed as the following equation:

$$\frac{Ce}{q_e} = \frac{1}{K_l \, x \, q_m} + \frac{Ce}{q_m}$$

where Ce is the equilibrium concentration of a metal ion, q_e is the adsorption capacity of the sorbent, q_m is the maximum adsorption capacity of the sorbent, and b is Langmuir constants.

While Freundlich isotherm adsorption models are expressed in the following equation:

$$\log Q_e = \log K_f + 1/n \log C_e$$

where n and K_f are the Freundlich constants.

Figure 11 shows the Langmuir and Freundlich adsorption

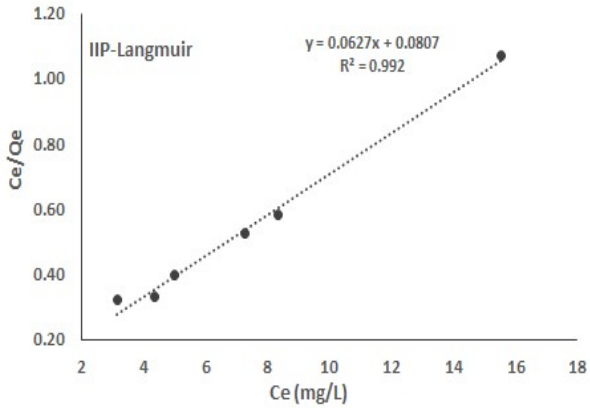

(a) Langmuir isotherm for Pb-IIP

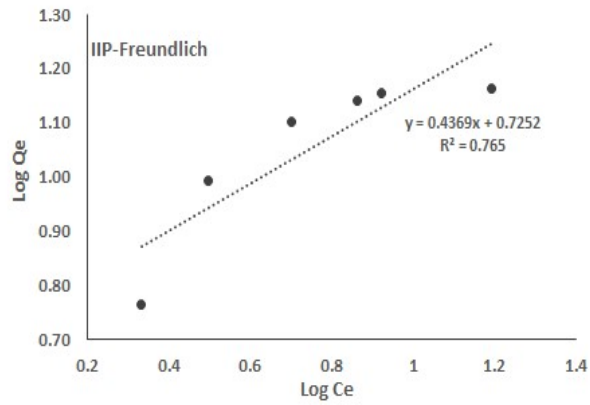

(b) Freundlich isotherm for Pb-IIP

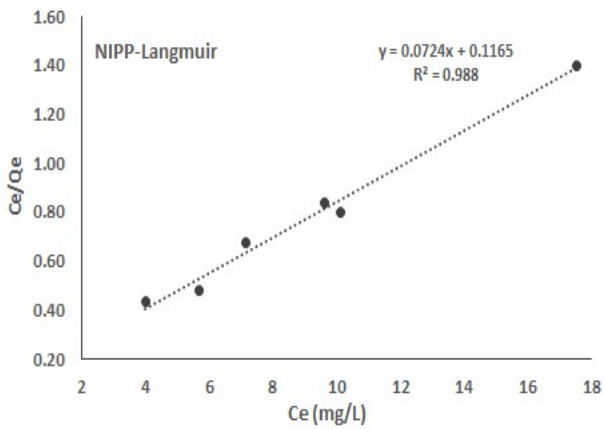

(c) Langmuir isotherm for NIPP

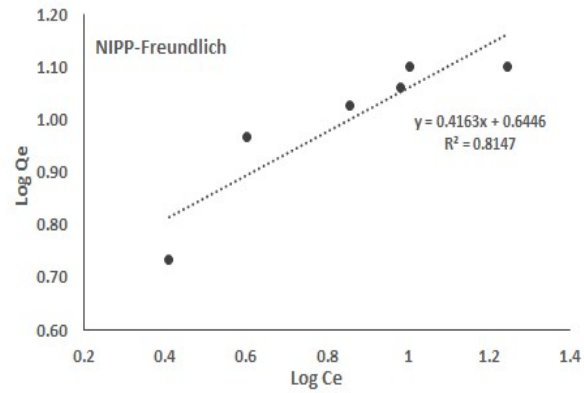

(d) Freundlich isotherm for NIPP

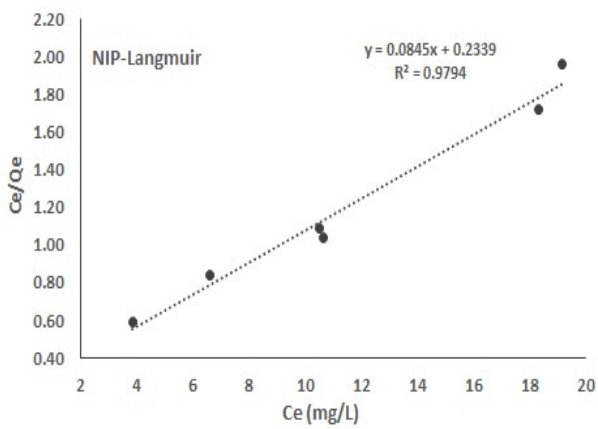

(e) Langmuir isotherm for NIP

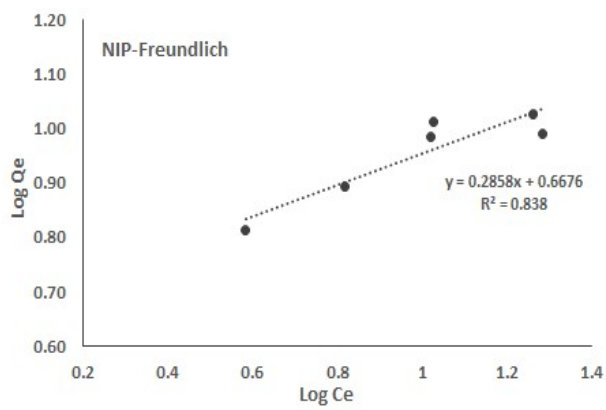

(f) Freundlich isotherm for NIP

Fig. 11. Langmuir isotherm and Freundlich isotherm model of Pb-IIP, NIPP, and NIP.

isotherm curves for Pb-IIP which show that R^2 values for Langmuir adsorption isotherms are 0.992. This value is better than the R^2 value on the Freundlich adsorption isotherm linear curve which shows the three sorbents following the Langmuir adsorption isotherm model. Table 3 also shows the parameters of each model for Pb-IIP sorbent which shows the

Table 3. Langmuir and Freundlich Adsorption Isotherm Model Parameters on Pb-IIP Sorbents from Linear Equations

Sorbent	Adsorption model									
	Langmuir					Freundlich				
	R^2	N	1/n	K	q_m	R^2	N	1/n	K	q_m
Pb-IIP	0.992			0.777	15.95	0.765	2.3	0.437	5.311	
NIPP	0.988			0.621	13.81	0.815	2.4	0.416	4.412	
NIP	0.979			0.621	11.83	0.838	3.5	0.286	4.652	

q_m value calculated on the Langmuir adsorption isotherm model is close to the experimental q_m value that reached 14.30 mg g^{-1} for Pb-IIP. Therefore, the Pb-IIP sorbent follows the Langmuir adsorption isotherm model which describes the type of monolayer adsorption on the sorbent surface which contains a limited number of recognition sites, while the Freundlich model assumes that adsorption occurs on heterogeneous or multilayer surfaces.

Kinetics Study

The study of adsorption kinetics was carried out by testing the data using pseudo-first order and pseudo-second order linear models which follow the equation:

$$\ln(q_e - q_t) = \ln q_e - k_1 t$$

$$\frac{t}{q_t} = \frac{t}{q_e} + \frac{1}{k_2\, q_e^2}$$

Q_e (mg g^{-1}) is the adsorption capacity at the equilibrium condition, q_t is the adsorption capacity of t time, K_1 and K_2 (g, mg^{-1}, min^{-1}) are the adsorption rate constant for pseudo-first order and pseudo-second order kinetics models.

The pseudo-order 1 model was tested by plotting between t (time) and log (Qe-Qt), while in the pseudo-order 2 model, plotting between t and Qe/t was made which produces the curves in Fig. 12 and Table 4. The R^2 value of the pseudo-order 2 model shows 0.999 which is greater than the R^2 value in the pseudo-order 1 model, which is only 0.964. This shows that the adsorption experimental results follow the pseudo-order 2 models. In addition, the q_e value of the pseudo-order 2 model of 12.0 mg g^{-1} is closer to the experimental q_e value of 11.82 mg g^{-1} compared to the calculated qe value of the pseudo-order 1 model which is only 4.08 mg g^{-1}. This result shows that the Pb-IIP sorbent follows the pseudo-second-order kinetics models that depend on the amount of the analyte and also the sorbent.

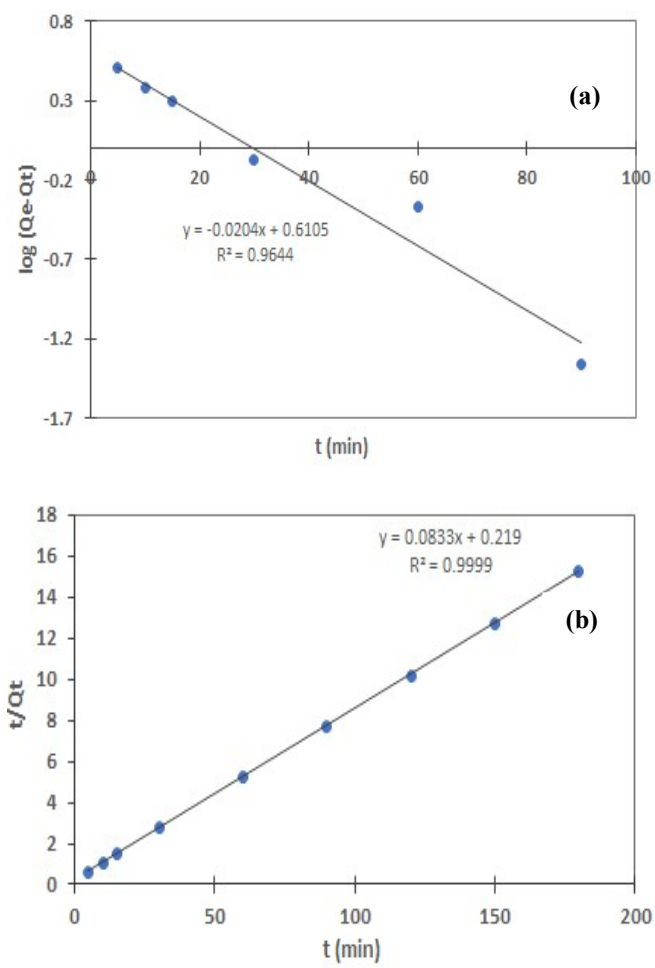

Fig. 12. (a) Pseudo first order (b) Pseudo second order kinetic model of Pb-IIP.

Table 4. Pseudo-order Kinetics Parameters of Order 1 and Order 2 on Pb-IIP Sorbent from a Linear Equation

Sorbent	Pseudo Order 1			Pseudo Order 2			
	K_1 (min^{-1})	R^2	q_e model ($mg\ g^{-1}$)	K_2 (min^{-1})	R^2	q_e model ($mg\ g^{-1}$)	q_{exp} ($mg\ g^{-1}$)
Pb-IIP	0.047	0.964	4.08	0.032	0.999	12.0	11.82

Table 5. Selectivity Data on Pb-IIP, NIPP, and NIP in the Quarternary Mixed Solution

Cation	Pb^{2+}	Cu^{2+}	Cd^{2+}	Zn^{2+}
Kd IIP ($l\ g^{-1}$)	3.39	0.17	0.08	0.08
Kd NIPP ($l\ g^{-1}$)	1.56	1.16	0.30	1.03
Kd NIP ($l\ g^{-1}$)	1.08	0.70	0.37	0.75
K IIP		19.99	42.96	42.15
K NIPP		1.35	5.23	1.51
K NIP		1.54	2.88	1.45
K' IIP/NIPP		14.82	8.21	27.90
K' IIP/NIP		13.02	14.91	29.12

Selectivity Study

Pb-IIP sorbents showed the ability to recognize Pb^{2+} ions compared to all other metal ions, especially in quaternary mixed solutions as indicated by the selectivity coefficient values shown in Fig. 13. Pb-IIP gave the highest selectivity coefficient values for Cd^{2+} reaching 42.96, Zn^{2+} 42.15, and Cu^{2+} 19.98.

Table 5 shows the distribution coefficient (Kd), relative selectivity coefficient (K'), and the selectivity coefficient K for Pb-IIP, NIPP, and NIP. The Kd values for the Pb-IIP were compared with NIPP and NIP which is greater for Pb^{2+} while decreased for Cu^{2+}, Cd^{2+}, and Zn^{2+}. This indicates that Pb-IIP has a better recognition ability of Pb^{2+} as a result of the imprinted ion template in the polymer sorbent.

The selectivity coefficient (k) of Pb-IIP for Pb^{2+}/Cu^{2+}, Cd^{2+}, and Zn^{2+} was found to be 19.99, 42.96, and 42.15 which is higher than NIPP and NIP. The high selectivity of Pb-IIP towards lead ion is due to strong complexation with PAR and 4-VP which provide specific binding sites for the target ion.

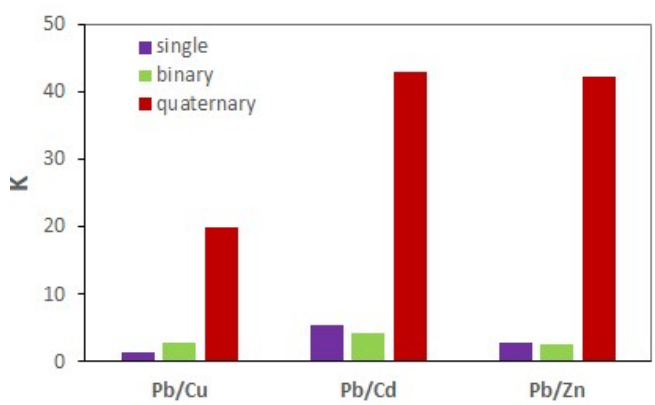

Fig. 13. Selectivity coefficient of Pb-IIP in single, binary, and quarternary solutions of Pb^{2+}, Cu^{2+}, Cd^{2+}, and Zn^{2+}.

Comparison with the Previous Study

The features of Pb-IIP in this study were compared to previously reported Pb-IIPs that were synthesized by various polymerization techniques as can be seen in Table 6. The comparison table shows that Pb-IIP synthesized by bulk polymerization based on ternary complex ion with PAR and 4-VP has an excellent selectivity even though the maximum adsorption capacity of this Pb-IIP is relatively smaller than some other sorbent.

Table 6. Comparison Table Between This Method and Literature

Monomer and/or ligand	Preparation technique	Maximum adsorption capacity (mg g^{-1})	Selectivity factors (k)	Ref.
MAA, 4-VP	Precipitation polymerization	25.30	16.2 (Pb^{2+}/Zn^{2+})	[13]
MAA, 4-VP	Suspension polymerization	8.40	17.36 (Pb^{2+}/Cu^{2+}), 26.53 (Pb^{2+}/Cd^{2+}), 29.84 (Pb^{2+}/Zn^{2+})	[43]
Diethyl amino ethyl methacrylate, 8-HQ	Precipitation polymerization	5.20	25.0 (Pb^{2+}/Cu^{2+}), 33.0 (Pb^{2+}/Cd^{2+}),	[19]
1-Vinyl imidazole, TMSPMA	Radical polymerization	7.60	2.80 (Pb^{2+}/Cu^{2+}), 50.0 (Pb^{2+}/Cd^{2+}), 7.5 (Pb^{2+}/Zn^{2+})	[6]
2-(Allyl sulfur) nicotinic acid	Precipitation polymerization	33.15	39.0 (Pb^{2+}/Cu^{2+}), 18.0 (Pb^{2+}/Cd^{2+})	[46]
HEMA, Styrene	Graft polymerization	38.50	4.52 (Pb^{2+}/Zn^{2+})	[47]
3-Aminopropyltrimethoxysilane (APS)	Surface imprinting technique on silica gel	19.66	49.3 (Pb^{2+}/Cd^{2+})	[48]
MAA, 4-VP, PAR	Bulk polymerization with ternary complex	14.30	19.99 (Pb^{2+}/Cu^{2+}), 42.96 (Pb^{2+}/Cd^{2+}), 42.15 (Pb^{2+}/Zn^{2+})	This study

Precision, Validation, and Application to Real Samples

Precisions of the method were assayed by conducting 5 replicates adsorption measurements of 20 mg l^{-1} of Pb^{2+} ion using 25 mg of Pb-IIP in inter-day time and the relative standard deviation percentage (%RSD) was calculated. According to the results, the % RSD for the precisions was to be 2.9% for the inter-day measurements.

Validation of the method was determined using a batch method to analyze real water samples including rainwater, tap water, and underground water. All the samples were collected from local sources that were chosen to be analyzed. Samples were adjusted to pH 6.0 and spiked with 2 mg l^{-1} of a Pb^{2+} standard solution. After batch experiments were conducted, the recovery of the samples with spiked and un-spiked was determined, the results are shown in Table 7. For all the spike samples the Pb-IIP showed high recoveries of the method between 97-103%. This value shows that in the adsorption of Pb^{2+} using Pb-IIP in the real samples there is no significant matrix interference. Based on the results, the high value of the recovery confirmed that the Pb-IIP can be used for the analysis of the Pb^{2+} ions in the real samples.

CONCLUSIONS

In this study lead ion imprinted polymer material (Pb-IIP) has been successfully synthesized by forming a ternary complex between Pb^{2+}, PAR ligands, and 4-VP with MAA, TRIM, and BPO as functional monomers, crosslinkers, and initiators. The synthesized Pb-IIP had a fairly good adsorption capacity of 14.52 mg g^{-1} compared to the control polymer (NIPP and NIP) at optimum conditions of pH 6, contact time of 120 min, and sorbent mass of 25 mg. The kinetics and isotherm of Pb-IIP adsorption followed the pseudo-order 2 and the Langmuir model. Pb-IIP polymer shows excellent selectivity towards other metal ions with Cu^{2+}, Zn^{2+}, and Cd^{2+} in a quaternary mixed solution with a selectivity coefficient for each metal ion reaching 19.98,

Table 7. Application of Pb-IIP to Analyze Rainwater, Tap Water, and Underground Water Spiked with 2 mg l^{-1} of a Standard Solution of Pb^{2+}, 25 mg Pb-IIP was Used in Solution pH 6, and Volume 15 ml

	C added (mg l^{-1})	C measured (mg l^{-1})	Recovery (%)
Rainwater	0	N.D	
	2	2.07	103.29
Tap water	0	N.D	
	2	1.95	97.60
Underground water	0	N.D	
	2	2.03	101.50

N.D = Not detected

42.15, and 42.96, respectively. The Pb-IIP also shows good precision and accuracy to use in real sample water that used in this work including rainwater, tap water, and underground water with the percentage of the recovery ranging from 97-103%.

ACKNOWLEDGMENTS

We would like to thank Beasiswa Saintek from the Ministry of Research and Technology Indonesia-BRIN for funding the doctoral degree and this dissertation research. Basic Sciences Center A laboratory ITB for the SEM-EDX analysis, Dr. Edi Pramono from Universitas Negeri Surakarta (UNS) for the TG-DTG analysis, Laboratory of Material Technology BPPT-BRIN for BET analysis, and Laboratory of Chemistry BRIN-Djunjunan for the rainwater samples supplied.

REFERENCES

[1] A. Abdullah, A. Balouch, F.N. Talpur, A. Kumar, M.T. Shah, A.M. Mahar, A. Amina, Microchem. J. 146 (2019) 1160.

[2] M.K. Bojdi, M.H. Mashhadizadeh, M. Behbahani, A. Farahani, S.S.H. Davarani, A. Bagheri, Electrochim. Acta 136 (2014) 59.

[3] X.-M. Zhan, X. Zhao, Water Res. 37 (2003) 3905.

[4] A.M. Basaglia, M.Z. Corazza, M.G. Segatelli, C.R.T. Tarley, RSC Adv. 7 (2017) 33001.

[5] C.R.T. Tarley, M.Z. Corazza, B.F. Somera, M.G. Segateli, J. Colloid Interface Sci. 450 (2015) 254.

[6] C.R.T. Tarley, F.N. Andrade, H.D. Santana, D.A.M. Zaia, L.A. Beijo, M.G. Segatelli, React. Funct. Polym. 72 (2012) 83.

[7] H. Ebrahimzadeh, M. Behbahani, Arab. J. Chem. 10 (2013) S2499.

[8] A.N. Anthemidis, Talanta 77 (2008) 541

[9] V. Boonamnuayvitaya, C.Y. Chaiya, W. Tanthapanichakoon, S. Jarudilokkul, Sep. Purif. Technol. 35 (2004) 11.

[10] M. Behbahani, A. Bagheri, M. Taghizadeh, M. Salarian, O. Sadeghi, L. Adinasab, K. Jalali, Food Chem. 138 (2013) 2050.

[11] M.G. Kakavandi, M. Behbahani, F. Omidi, G. Hesam, Food Anal. Methods 10 (2017) 2454.

[12] G. Yang, W. Fen, C. Lei, W. Xiao, H. Sun, J. Hazard. Mater. 162 (2009) 44.

[13] Y. Jiang, B. Tang, P. Zhao, M. Xi, Y. Li, J. Inorg. Organomet. Polym. 31 (2021) 4628.

[14] M. Behbahani, S. Salimi, H.S. Abandansari, F. Omidi, M. Salarian, A. Esrafili, RSC Adv. 5 (2015) 59912.

[15] C.F. Poole, Trac Trends Anal. Chem. 22 (2003) 362.

[16] P.G. Krishna, J.M. Gladis, T.P. Rao, G.R. Naidu, J. Molec. Recog. 18 (2005) 109.

[17] E. Yilmaz, M. Soylak, Talanta 158 (2016) 152.

[18] M. Rammika, G. Darko, Z. Tshentu, J. Sewry, N. Torto, Water SA. 37 (2011) 321.

[19] N. Garcia-Otero, C. Teijeiro-Valino, J. Otero-Romani, E. Pena-Vazquez, A. Moreda-Pineiro, P. Bernejo-Barrera, Anal. Bioanal. Chem. 395 (2009) 1107.

[20] G. Wuff, T. Gross, R. Schonfeld, T. Schrader, C. Kristen, in: R.A. Bartsch, M. Maeda (Eds.), American Chem. Soc., 1998.
[21] H. Nishide, J. Deguchi, E. Tsuchida, Chem. Lett. 2 (1976) 169.
[22] P.E. Hande, A.B. Samui, P.S. Kulkarni, Enviro. Sci. Pollut. Res. 22 (2015) 7375.
[23] A. Kumar, A. Balouch, Abdullah, A.A. Pathan, Polym. Test. 77 (2019) 105871.
[24] F.A. Mustafai, A. Balouch, Abdullah, N. Jalbani, M.I. Bhanger, M.S. Jagirani, A. Kumar, A. Tunio, European Polym. J. 109 (2018) 133
[25] F. Shakerian, K.H. Kim, E. Kwon, J.E. Szulejko, P. Kumar, S. Dadfarnia, A.M.H. Shabani, Trac Trends Anal. Chem. 83 (2016) 55.
[26] L. Mergola, S. Scorrano, E. Bloise, M.P.D. Bello, M. Catalano, G. Vasapollo, R.D. Sole, Polym. J. (2015) 1.
[27] C. Branger, W. Meouche, A. Margaillan, React. Funct. Polym. 73 (2013) 28.
[28] Y.K. Tsoi, Y.M. Ho, K.S.Y. Leung, Talanta 89 (2012) 162.
[29] T.P. Rao, R. Kala, S. Daniel, Anal. Chim. Acta 578 (2006) 105.
[30] F. Masoumi, P. Sarabadani, A.R. Khorrami, Polym. Bull. 76 (2019) 5499.
[31] M. Moussa, V. Pichon, C. Mariet, T. Vercouter, N. Delaunay, Talanta 161 (2016) 459.
[32] S. Mishra, D.K. Singh, Desalin. Water Treat. 56 (2014) 1364.
[33] V.E. Pakade, E.M. Cukrowska, J. Darkwa, G. Darko, N. Torto, Water Sci. Technol. 65 (2012) 728.
[34] D. James, G. Venkateswaran, T.P. Rao, Micro. Meso. Materials 119 (2009) 165.
[35] R. Kala, T.P. Rao, J. Sep. Sci. 29 (2006) 1281.
[36] R. Kala, J.M. Gladis, T.P. Rao, Anal. Chim. Acta 518 (2004) 143.
[37] P. Metilda, J.M. Gladis, T.P. Rao, Anal. Chim. Acta 512 (2004) 63.
[38] M.S. Sastry, R. Ghose, A.K. Ghose, Bull. Chem. Soc. Ethiop. 4-1 (1990) 61.
[39] A. Kocyla, A. Pomorski, A. Krezel, J. Inorg. Biochem. 152 (2015) 82.
[40] S. Daniel, R.S. Praveen, T.P. Rao, Anal. Chim. Acta 570 (2006) 79.
[41] S. Asman, S. Mohammad, N.M. Sarih, Int. J. Mol. Sci. 16 (2015) 3656.
[42] M. Grochowicz, J. Therm. Anal. Calorim. 118 (2014) 1603.
[43] X. Cai, J. Li, Z. Zhang, F. Yang, R. Dong, L. Chen, ACS Appl. Mater. Interfaces 6 (2014) 305.
[44] Y. Isikver, S. Baylav, Bull. Mater. Sci. (2018) 41.
[45] P. Girija, M. Beena, Sep. Sci. Tech. 49 (2014) 1053.
[46] X. Ao and H. Guan, Ads. Sci. Tech. 36 (2017) 774.
[47] X. Luo, H. Yu, Y. Xi, L. Fang, L. Liu, J. Luo, RSC Adv. 7 (2017) 25811.
[48] X. Zhu, Y. Cui, X. Chang, X. Zou, Z. Li, Microchim. Acta 164 (2009) 125.